Sorting Rotating Micromachines by Variations in Their Magnetic Properties

Taylor A. Howell,[1,2] Braxton Osting,[3] and Jake J. Abbott[1,4]

[1]*Department of Mechanical Engineering, University of Utah, Salt Lake City, Utah 84112, USA*
[2]*Department of Mechanical Engineering, Stanford University, Stanford, California 94305, USA*
[3]*Department of Mathematics, University of Utah, Salt Lake City, Utah 84112, USA*
[4]*Robotics Center, University of Utah, Salt Lake City, Utah 84112, USA*

(Received 2 October 2017; revised manuscript received 1 December 2017; published 16 May 2018)

We consider sorting for the broad class of micromachines (also known as microswimmers, microrobots, micropropellers, etc.) propelled by rotating magnetic fields. We present a control policy that capitalizes on the variation in magnetic properties between otherwise-homogeneous micromachines to enable the sorting of a select fraction of a group from the remainder and prescribe its net relative movement, using a uniform magnetic field that is applied equally to all micromachines. The method enables us to accomplish this sorting task using open-loop control, without relying on a structured environment or localization information of individual micromachines. With our method, the control time to perform the sort is invariant to the number of micromachines. The method is verified through simulations and scaled experiments. Finally, we include an extended discussion about the limitations of the method and address open questions related to its practical application.

DOI: 10.1103/PhysRevApplied.9.054021

I. INTRODUCTION

There has been substantial effort from the research community working toward the goal of enabling wirelessly controlled magnetic micromachines (also known as microswimmers, microrobots, micropropellers, etc.) to be used in biomedical applications [1–3]. To date, research on the control of magnetic micromachines has typically considered a single micromachine [4–6], a very small set of micromachines that are individually localized [7–13], or a group of micromachines (sometimes referred to as a "swarm") that are controlled as an aggregate unit with no ability to differentiate individual micromachines [14–16]. For clinical use, a medical image will likely show a group as a cloud in the image [15], and it may be unrealistic to assume that each micromachine can be individually localized and controlled. In addition to the localization problem, each micromachine in the group will be subjected to the same applied magnetic field, and spatial changes in that field over a tightly packed group will likely be small for *in vivo* applications, making it challenging to differentiate the actuation being applied to the micromachines by utilizing spatial variations in the field. Although these represent significant challenges, it may be desirable—or even necessary for certain applications—to perform basic manipulation of a group beyond simply moving the group as an aggregate.

In this paper, we show how knowledge of magnetic variation can be exploited to sort a group of otherwise-homogeneous micromachines, even in a uniform magnetic field in which all micromachines are actuated by a single input. By *sort*, we mean to separate away a desired fraction of the original group to form two new distinct subgroups. We consider the broad class of micromachines that convert magnetic torque generated by a rotating magnetic field into propulsion, which includes using both chiral (e.g., helical) and achiral structures to swim or screw through fluids and soft tissues, as well as devices that roll on a surface. This class of micromachine has been well studied and has been shown to have desirable scaling properties for biomedical applications when compared to other micromachine types [17]. Our vision is that a group of micromachines could be fabricated with engineered variation in their magnetic properties purely for the purpose of enabling sorting (potentially by simply relaxing process control during fabrication), using micromachine designs in which variation in magnetic properties can be introduced without adding significant variation to the geometric parameters to which propulsion is sensitive.

A number of prior works have proposed using heterogeneity among micromachines to control groups with uniform global inputs. Much of this prior work has considered only a relatively small number of micromachines. Two helical micromachines with distinct geometries and/or magnetic properties have been shown to exhibit unique velocity responses to a uniform field [18,19]. The similarly differentiated responses of three geometrically distinct microrobots to a global input were learned and subsequently controlled [7]. Another study experimentally confirmed differentiated behavior, produced by a global magnetic field, in two heterogeneous

three-bead micromachines known as achiral swimmers [20]. Work by our group characterized the behavior of magnetic micromachines when operated at frequencies above their step-out frequency and explored how variation in the step-out frequency in geometrically identical micromachines differentiates the micromachines' relative velocity responses [21]. Magnetic field gradients have been used to uniquely control geometrically or magnetically heterogeneous micromachines in 3D [8]; this method can be implemented in an open-loop fashion and can be scaled to control an arbitrary number of micromachines, but control authority reduces as the number of micromachines increases and current hardware is limited to full independent control of two micromachines. Specialized substrates that "anchor" or locally manipulate micromachines have experimentally demonstrated independent control of multiple micromachines [22]; this technique is potentially well suited for microassembly tasks, but it is not a practical solution for *in vivo* medical applications.

Other prior works have utilized heterogeneity among micromachines to sort large groups of an arbitrary number. In a work particularly related to ours, differentiation in velocity responses was used to sort irregular achiral "nanopropellers" by size, utilizing the correlation between size and magnetic strength [23]. It is also possible to sort a group of chiral swimmers into two distinct subgroups of left- and right-handed chirality [24].

Other related work has considered how to sort microswimmers using specialized microfluidic channel geometries. Chiral microswimmers have been sorted according to chirality, linear velocity, and angular velocity using patterned microstructures [25]; an environment with physical impediments was designed to selectively restrict swimmer motion according to a particular swimmer property. Shear flow has also been used to separate chiral objects [26]. For micromachines, a microfluidic environment could be used to presort and reject defective micromachines and more easily group similar micromachines prior to *in vivo* applications. However, the physical environment will ultimately preclude such methods from use during *in vivo* medical applications.

Other work has considered control policies that go beyond simple sorting for groups with an arbitrary number, and a continuous ensemble, of devices that receive identical inputs but generate unique forward speeds. Such studies from the robotics literature have typically relied on a closed-loop feedback policy or are dependent upon localization information [27,28] and, as a result, are infeasible for the biomedical applications of interest here. One prior work particularly related to ours described a method to independently control an arbitrary number of micromachines with variations in magnetic and/or hydrodynamic properties, provided that the properties are known [11]; this method can also be applied open loop. Another study showed how variation in the direction (as opposed to the strength) of the magnetization with respect to the otherwise-homogeneous micromachines' bodies can be used to differentiate control [10]. With all of the above methods, the control time tends to increase with an increase in the number of micromachines.

In this paper, we provide a method to sort some desired fraction of micromachines from the rest of the group by driving the entire group in a given desired direction using a constant frequency of the rotating magnetic field, which spreads the group out similar to Ref. [23] (we refer to this as the separation process), and by then driving the entire group in the reverse direction using a time-varying frequency function that collects the micromachines into two distinct groups (we refer to this as the collection process), as depicted in Fig. 1. Upon the conclusion of this open-loop separation-collection cycle, there is a net forward movement of the fraction of the group that we have chosen to sort, and there is no net movement in the remaining group (similar to Ref. [10]). The separation-collection cycle can be repeated to continue to make forward progress of the

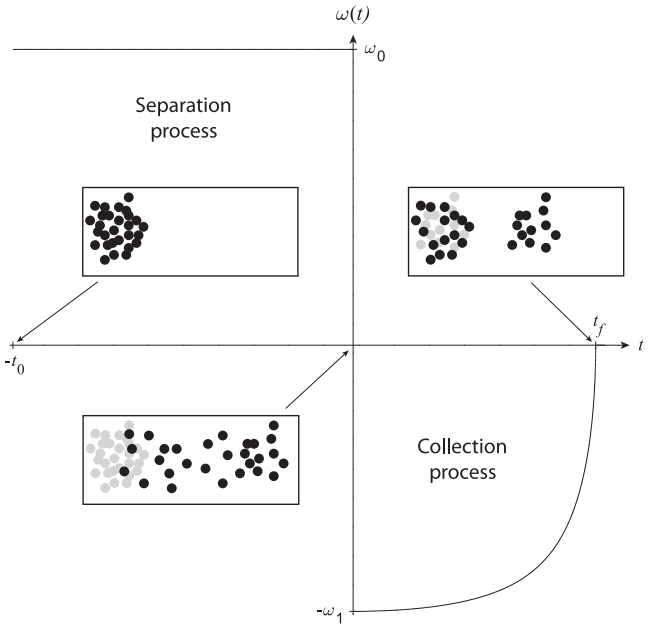

FIG. 1. Proposed sorting process. In this separation-collection cycle, a time-varying frequency of a rotating uniform magnetic field is used to sort a group into two distinct subgroups. After a constant-frequency separation process of frequency ω_0 and duration t_0, the individual micromachines are differentiated in displacement according to their step-out frequencies. Following a collection process that reverses direction and begins at a frequency $\omega_1 < \omega_0$, the desired fraction of the group is sorted, making net forward movement while the remainder of the group returns to the original starting position. We choose to establish $t = 0$ as the transition from the separation process to the collection process because this paper is largely focused on developing the collection process. Note that the dots used to represent the micromachines are not necessarily to scale with their relative separation.

sorted group without any net movement of the original group. To form more than two groups, the original group (i.e., the micromachines left behind during the sort) or the sorted group can be further subdivided without any net disturbance of the previous group(s). This process naturally leads to a motion-planning method for a group of micromachines. Our approach to micromachine differentiation relies on neither localization of individual micromachines nor a structured environment. In addition, our approach does not require knowledge of the number of micromachines and is invariant to the number of micromachines in terms of the control time required to perform a sort, which distinguishes it from related prior works [10,11]. However, our method relies on an assumption that the micromachines have variation in their magnetic properties but have homogeneous hydrodynamic properties, which is less general than the assumptions of Ref. [11].

II. REVIEW OF MODELS OF ROTATING MICROMACHINES

We assume the commonly used low-Reynolds-number swimming model in which a chiral microswimmer can rotate about, and translate along, its axis [29]. After a rearrangement of terms from Ref. [29] as described in Ref. [17], an individual microswimmer is modeled as

$$\begin{bmatrix} v \\ \tau \end{bmatrix} = \begin{bmatrix} \alpha & \beta \\ -\beta & \gamma \end{bmatrix} \begin{bmatrix} f \\ \omega \end{bmatrix}, \tag{1}$$

where ω is the angular velocity of the applied field, which is also referred to as the field rotation frequency, and it is assumed that the microswimmer rotates about its axis synchronously with the applied field (we will return to this assumption); f is any externally applied (nonfluidic) force applied along the axis of the microswimmer; v is the translational velocity along the axis; τ is the (nonfluidic) torque that is being generated on the microswimmer about its axis to cause ω; and the parameters α, β, and γ encapsulate the relevant properties of the microswimmer's geometry and the environment. Note that, although the input and output terms are vectors in general, this common simplified axial-swimming model considers only the magnitude of those vectors. The microswimmer is assumed to have negligible inertia. Since a uniform field does not vary spatially, there are no magnetic forces acting on the microswimmer; we also assume that the forces of gravity are negligible relative to other effects (gravitational effects are discussed more later). As a result, the model equation (1) can be simplified as

$$\begin{bmatrix} v \\ \tau \end{bmatrix} = \begin{bmatrix} \beta \\ \gamma \end{bmatrix} \omega. \tag{2}$$

The same model from Eq. (2) also applies to magnetic micromachines that roll. The principal difference between a microswimmer and a rolling micromachine is that, in the case of the microswimmer, the velocity vector tends to be parallel with the angular velocity vector, whereas with a rolling micromachine the two vectors tend to be orthogonal. However, since Eq. (2) considers only the magnitudes of the respective vectors, it applies to both types of micromachines for our purposes.

A given micromachine, in a given magnetic field, will have a maximum torque, $\tau_{\max}$, that can possibly be generated. When the applied magnetic field rotates sufficiently slowly such that the torque calculated from Eq. (2) is achievable (i.e., $\tau \leq \tau_{\max}$), the micromachine synchronously rotates with the field, and its forward velocity is proportional to the angular velocity of the applied field. There exists a field rotation frequency, however, above which the available magnetic torque is not strong enough to keep the micromachine rotating synchronously with the field, which is typically referred to as the "step-out" frequency ω_{so} [18], where $\omega_{so} = \tau_{\max}/\gamma$, but has also been referred to as the "critical frequency" [23]. At field rotation frequencies above the step-out frequency, the linear model in Eq. (2) is invalid.

The average angular velocity of a micromachine, $\bar{\omega}_m$, as a function of the field rotation frequency, ω, has been solved in closed form for both permanent-magnet and soft-ferromagnetic micromachines with a variety of geometries [30–34]:

$$\bar{\omega}_m = \begin{cases} \omega, & \omega \leq \omega_{so} \\ \omega - \sqrt{\omega^2 - \omega_{so}^2}, & \omega > \omega_{so} \end{cases}. \tag{3}$$

Once $\bar{\omega}_m$ is found, Eq. (2) can be used to calculate the translational velocity as $v = \beta\bar{\omega}_m$. This phenomenon has been experimentally verified using microswimmers [21,23,24,30] and rolling machines with Reynolds-number scaling to simulate microscale devices [21], and it has been found to be a good predictor of observed behavior.

III. DEVELOPMENT OF THE SORTING PROCESS

Utilizing the phenomenon of Eq. (3), introducing variation in the magnetic properties within a group (i.e., changing ω_{so} for each micromachine) leads to three operating modes: a homogeneous mode where all micromachines respond identically to the rotating magnetic field, a heterogeneous mode where each micromachine responds uniquely according to its step-out frequency, and a hybrid mode where a fraction of the group operates homogeneously and the remainder operates heterogeneously. For example, consider a group of ten geometrically identical micromachines with variations in their magnetic properties, with velocity responses shown in Fig. 2, whose step-out frequencies are distributed regularly throughout an interval with the step-out frequency of the weakest one

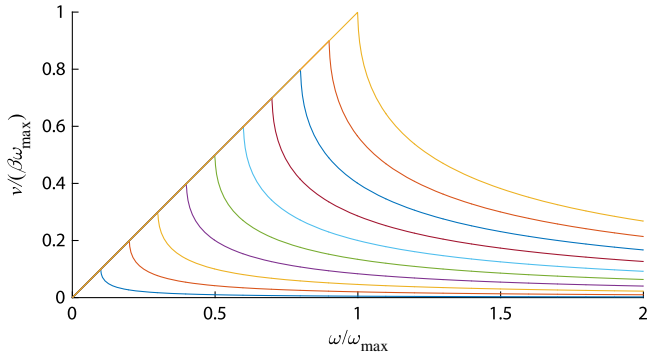

FIG. 2. Nondimensionalized velocity responses of ten micromachines having identical geometries and regularly spaced step-out frequencies $\omega_{so}/\omega_{max} \in [0.1, 1]$. The step-out frequency can be seen as the frequency ω at which the velocity v starts decreasing with an increase in ω.

being only 10% of the step-out frequency of the strongest one: $\omega_{min} = 0.1\omega_{max}$. Rotating the field at a frequency $\omega < \omega_{min}$ produces homogeneous responses among micromachines, causing them to move in unison with no change in their relative positions; this is the most basic group-manipulation primitive. Rotating the field at a frequency $\omega_{min} < \omega < \omega_{max}$ results in a hybrid response, resulting in speed differentiation in a fraction of the group and a faster homogeneous speed in the remaining fraction; we utilize this regime in the design of the sorting primitive.

As we consider large numbers of micromachines within a group, we assume that their step-out frequencies can be described by some distribution (e.g., uniform, Gaussian), with a minimum and maximum step-out frequency, ω_{min} and ω_{max}, respectively (Fig. 3). It is not important what the distribution is, simply that its parameters are known. Using the cumulative distribution function, we can find a field rotation frequency ω_0 such that some desired fraction of the group has step-out frequencies higher than ω_0 (this is the fraction that we sort, which we refer to as the *fast* group), and the remaining micromachines (which we refer to as the *slow* group) have step-out frequencies below ω_0.

We find that, for our method to be practical, we must allow some small fraction of the nonfast group to have an unspecified amount of net movement (although it will never be as large as that of the fast group). We specify a frequency $\omega_1 < \omega_0$, such that all micromachines with $\omega_{so} \leq \omega_1$ have no net movement, but micromachines with $\omega_1 < \omega_{so} < \omega_0$ are *sacrificed* by not truly belonging to the slow group. We again use the cumulative distribution function (Fig. 3) to choose ω_1 to correspond to a given fraction of the group that we are willing to sacrifice. In the limit as $\omega_1 \to \omega_0$ (i.e., we are not willing to sacrifice any micromachines), the collection process trivially mirrors the separation process, and there is no net movement of the fast group relative to the slow group.

The separation process rotates the uniform magnetic field at a single frequency for a duration t_0, after which the

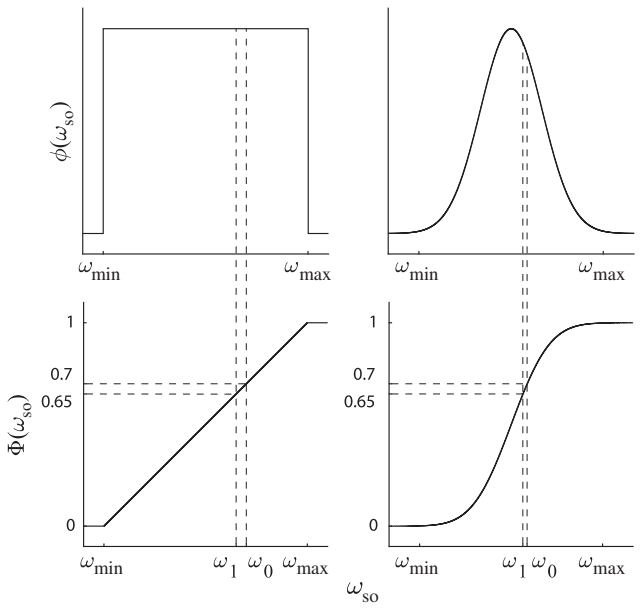

FIG. 3. Distribution of magnetic properties. (Top panels) Probability density function for a distribution of step-out frequencies with (bottom panels) associated cumulative distribution function for (left panels) a uniform distribution and (right panels) a Gaussian distribution. In both cases shown, ω_0 is selected to sort the fastest 30% of the group, and ω_1 is selected to sacrifice 5% of the group as belonging to neither the fast nor the slow group. In the case of the Gaussian distribution, ω_{max} and ω_{min} are chosen to correspond to the $\pm 3\sigma$ values of the distribution.

fast micromachines (i.e., those with $\omega_{so} \geq \omega_0$) will have traveled a distance d_0:

$$d_0 = \beta t_0 \omega_0, \tag{4}$$

while slow and sacrificed micromachines (i.e., those with $\omega_{so} < \omega_0$) will have traveled distances less than d_0, depending upon their step-out frequencies. Equation (4) is simply the integral of the velocity component of Eq. (2) over the separation process for the fast micromachines. In practice, we would likely use Eq. (4) to select t_0 for a given d_0 (i.e., the maximum micromachine displacement from the origin) that we are willing to allow in a single separation-collection cycle; a similar "excursion" is described in Ref. [11]. However, we should also choose a large enough t_0 to allow multiple rotation cycles since Eq. (3) is derived under an assumption of steady-state rotation.

The complete separation-collection cycle is characterized by three parameters: the separation-process frequency ω_0, the separation-process duration t_0, and the initial collection-process frequency ω_1 (Fig. 1). Selection of these three parameters provides control over the size of the two new groups (including the fraction of sacrificed micromachines) and the final separation distance between the two new groups. Once these three parameters are selected, our time-varying collection process is well defined. These

parameters are determined from the statistical variation in the group and the desired net forward movement of the fast group. The descending-frequency collection process is unique given a constant-frequency separation process.

The collection process is a time-varying frequency function $\omega(t)$, subject to $\omega(t) < \omega_0$ for $t \geq 0$, that satisfies the equality

$$t_0\left(\omega_0 - \sqrt{\omega_0^2 - \omega_{\mathrm{so}_i}^2}\right) = \int_0^{t_{\mathrm{so}_i}} \left(\omega(s) - \sqrt{\omega(s)^2 - \omega_{\mathrm{so}_i}^2}\right) ds + \int_{t_{\mathrm{so}_i}}^{t_f} \omega(s) ds \tag{5}$$

for each micromachine in the slow group (i.e., for each $\omega_{\mathrm{so}_i} \leq \omega_1$). The left-hand side of Eq. (5) is the distance a slow micromachine with step-out frequency ω_{so_i} travels during the separation process, defined as the integral of Eq. (2) but using the correct average angular velocity from Eq. (3), over the separation process. The right-hand side of Eq. (5) is the distance traveled by the same micromachine during the collection process, comprising the distance traveled when the micromachine rotates out of synchronization and in synchronization with the applied field [integrating Eq. (2) as before, but over two distinct intervals during the collection process]. The duration of the collection process, t_f, is always less than t_0. The time t_{so_i} is unknown; it is the duration that a micromachine with step-out frequency ω_{so_i} rotates out of synchronization with the field during the collection process, such that $\omega(t_{\mathrm{so}_i}) = \omega_{\mathrm{so}_i}$.

A function that satisfies Eq. (5) is defined by

$$\omega(t) = \begin{cases} \omega_1, & t \in [0, t_1) \\ \omega_k, & t \in \left[\sum_{j=1}^{k-1} t_j, \sum_{j=1}^{k} t_j\right), \end{cases} \qquad 1 < k < n, \tag{6a}$$

$$\omega_k = \omega_1 - \left(\frac{k-1}{n-1}\right)\omega_1, \qquad 1 \leq k < n, \tag{6b}$$

$$t_1 = \frac{t_0\left(\sqrt{\omega_0^2 - (\omega_1 - \frac{1}{n-1}\omega_1)^2} - \sqrt{\omega_0^2 - \omega_1^2}\right)}{\sqrt{\omega_1^2 - (\omega_1 - \frac{1}{n-1}\omega_1)^2}}, \tag{6c}$$

$$t_k = \frac{t_0\left(\sqrt{\omega_0^2 - (\omega_1 - \frac{k}{n-1}\omega_1)^2} - \sqrt{\omega_0^2 - \omega_1^2}\right)}{\sqrt{(\omega_1 - \frac{k-1}{n-1}\omega_1)^2 - (\omega_1 - \frac{k}{n-1}\omega_1)^2}} - \frac{\sum_{j=1}^{k-1} t_j\left(\sqrt{(\omega_1 - \frac{j-1}{n-1}\omega_1)^2 - (\omega_1 - \frac{k}{n-1}\omega_1)^2}\right)}{\sqrt{(\omega_1 - \frac{k-1}{n-1}\omega_1)^2 - (\omega_1 - \frac{k}{n-1}\omega_1)^2}}, \quad 1 < k < n, \tag{6d}$$

where a series of steplike operations at a constant frequency ω_k for a duration t_k are assembled to approximate a continuous function, provided an appropriate number of steps (e.g., $n \gg 100$).

The numerical solution in Eq. (6) describes the physical process of "collecting" micromachines one after another following the separation process. In the development of the collection process, a continuous distribution of step-out frequencies is first approximated by a finite set of known step-out frequencies. The collection process is then generated as a series of operations, each performed at a constant frequency ω_i for a duration t_i, with the goal of collecting the micromachines in the slow group together one by one while keeping the fast group moving homogeneously, and disregarding what happens to the sacrificed micromachines. The collection process creates a new homogeneous group within the slow group, starting with the single micromachine with the highest step-out frequency. In each operation, this homogeneous group is driven at a frequency ω_i corresponding to the lowest step-out frequency of any micromachine in the homogeneous group, resulting in the homogeneous group eventually overtaking (i.e., collecting) the micromachine with the next-highest step-out frequency, at which point it becomes part of the homogeneous group. This process is iterated with descending frequencies until all of the slow micromachines are collected into a single homogeneous group, at which time the entire slow group is moved homogeneously the remaining distance to the origin (i.e., the location before the separation process is initiated). The duration t_i to operate at ω_i is

$$t_i = \frac{x_i - x_{i+1}}{v_i - v_{i+1}}, \tag{7}$$

where the index i denotes descending step-out frequencies of micromachines in the slow set, and x_i and v_i are the current position and velocity, respectively, of a micromachine with step-out frequency ω_{so_i}. Equation (7) is the general form of Eqs. (6c) and (6d). For the final operation to return to the origin, we collect a theoretical micromachine having $\omega_{\mathrm{so}} = 0$. The series of ω_i, t_i operations is assembled to form the piecewise collection-process function, $\omega(t)$.

Consider n micromachines with identical β values and $\omega_{\mathrm{so}}/\omega_{\mathrm{max}}$ equally spaced in the range [0,1]. Using a given set of the three key parameters, an n-micromachine collection process using Eq. (6) approximates a continuous function as $n \to \infty$, as seen in Fig. 4. In practice, when n is sufficiently large (e.g., $n = 1000$), the approximation can be applied successfully as a cycle's collection process. Although the methodology used to derive the collection process requires knowledge of the individual micromachines' step-out frequencies, the continuous collection process found by the methodology no longer requires that knowledge. Rather, it sweeps through every possible step-out frequency that may exist within the group. In the Appendix, we show that the continuous collection process

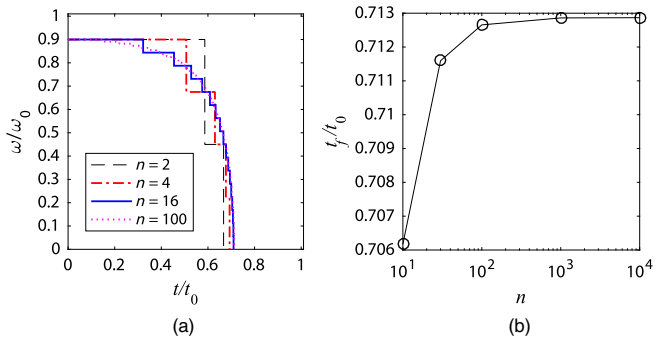

FIG. 4. Development of discrete collection process as n increases. (a) Series of operations, initiated with $\omega_1/\omega_0 = 0.9$, to collect n micromachines. The piecewise function converges to a continuous function as $n \to \infty$, satisfying Eq. (5). (b) The total time required to collect n micromachines also converges. The value to which t_f/t_0 converges is unique for the selection of ω_1/ω_0 (see Fig. 5).

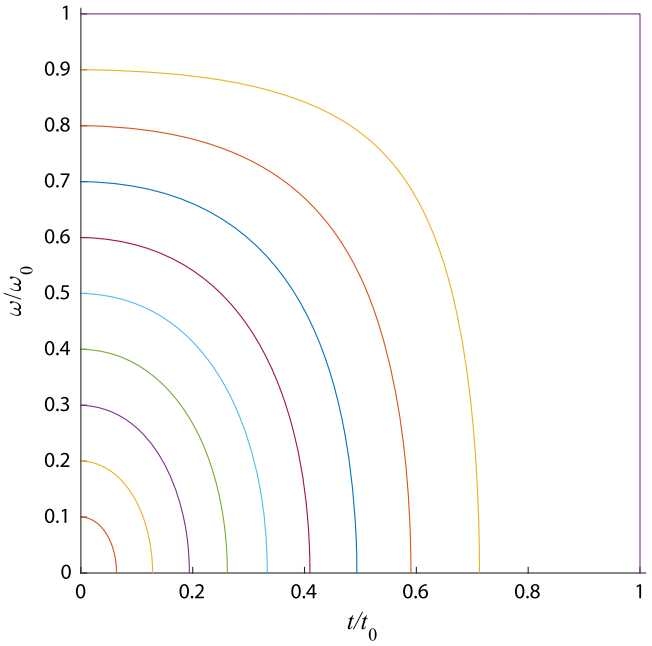

FIG. 5. Ten nondimensional collection-process functions, where each curve corresponds to a unique ω_1/ω_0 regularly spaced in the set [0.1,1], and $\omega = \omega_1$ at $t = 0$.

found with this method is unique (given a constant-frequency separation process). The collection-process function, with a frequency decreasing from ω_1 to 0 over a duration always less than t_0, can be normalized with respect to the time t_0 and the frequency ω_0. A set of such normalized processes is assembled in Fig. 5.

IV. NUMERICAL AND EXPERIMENTAL VERIFICATION

A complete separation-collection cycle is depicted in Fig. 6. After the collection process, the fast group has a net forward displacement of distance d:

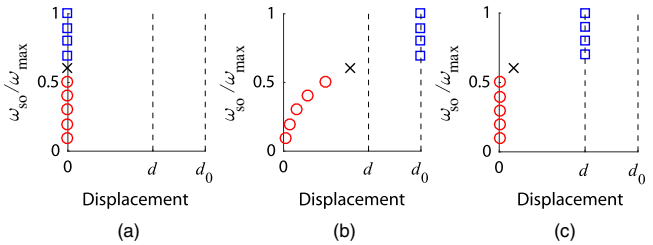

FIG. 6. Implementation of a separation-collection cycle with an idealized ten-micromachine group from a uniform distribution. The step-out frequencies of the individual micromachines are depicted graphically. Fast micromachines are denoted by blue squares, slow micromachines by red circles, and sacrificed micromachines by black crosses. The velocity responses of these ten micromachines are depicted in Fig. 2. (a) Initial micromachine positions are identical. (b) Micromachine displacement after the separation process with $\omega_0/\omega_{\max} = 0.7$. (c) Micromachine displacement after the collection process initiated with $\omega_1/\omega_{\max} = 0.5$.

$$d = \beta t_0 \sqrt{\omega_0^2 - \omega_1^2}, \tag{8}$$

while the slow group has no net displacement. Equation (8) is the difference in positions of micromachines with step-out frequencies ω_0 and ω_1 following the separation process [i.e., $d = d_0 - d_1 = \beta t_0 \omega_0 - \beta t_0(\omega_0 - \sqrt{\omega_0^2 - \omega_1^2})$]. In practice, once an allowable d_0 is set using Eq. (4), we use Eq. (8) to determine the number of times the separation-collection cycle must be repeated in order to produce the desired net movement of the fast group.

Consider a large group of micromachines randomly selected from a population with identical geometries and a Gaussian distribution of step-out frequencies, uniformly distributed in a spherical volume to assist in visualization. Such a group appears as a cloud, as depicted in Fig. 7. Say that we wish to sort 30% of the original group, leaving 65% behind, and we are willing to sacrifice 5% as belonging firmly to neither group. Based on the population's distribution of magnetic properties, the separation-collection cycle is implemented using the methods described above. The separation-collection cycle does not reduce the initial disorder, but postcycle we see that the separation-collection cycle is not affected by the group's initial internal arrangement. The original group has been sorted into two distinct groups. The relationship between d and d_0 is determined by the selection of ω_0 and ω_1. To increase the total displacement of the fast group, the cycle should be repeated.

To experimentally verify the sorting policy, a group of three rolling mesomachines is fabricated [Fig. 8(a)]. Each device is fabricated from a (nonmagnetic) aluminum rod and measures 3 mm in diameter and 8 mm in length. To make each device magnetically distinct, one, two, or three holes are drilled perpendicular to the axis of symmetry, with 0.82-mm-diameter (soft-magnetic) Permalloy 80

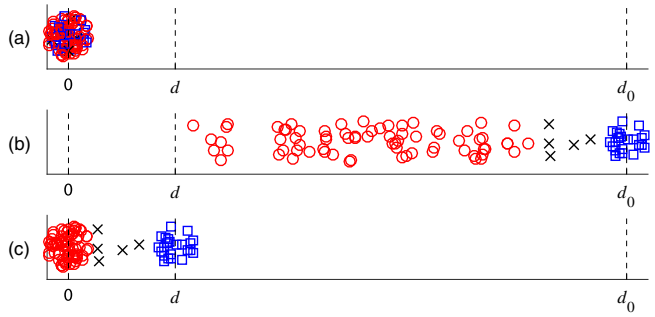

FIG. 7. Implementation of a separation-collection cycle with a micromachine group from a Gaussian distribution. The group comprises 100 micromachines sampled from a population with identical geometries and a distribution of step-out frequencies $\omega_{so}/\omega_{max} \sim \mathcal{N}(0.7, 0.01)$. The fast group is denoted by blue squares, the slow group by red circles, and sacrificed micromachines by black crosses. Axes correspond to Cartesian position coordinates, simulating what would be seen in a medical image. (a) The initial group, with micromachines randomly assigned in a circle approximating a medical image cloud (e.g., after a bolus injection of micromachines). (b) Micromachine positions after a separation process with $\omega_0/\omega_{max} = 0.752$ and $t_f/t_0 = 0.877$. (c) Final positions of the new fastest 30% and slowest 65% groups, separated by an average nondimensionalized distance $d/(\beta t_0 \omega_{max}) = 0.144$, following the separation-collection cycle initiated with $\omega_1/\omega_{max} = 0.738$.

wires of approximately the same length inserted and glued into each hole. These devices are operated in a fluid medium comprising a 2:1 mixture of corn syrup and water, selected to achieve desirable temporal and spatial characteristics to demonstrate sorting, while reducing the Reynolds number to simulate micromachines of approximately 1/50 the size in water.

A rotating uniform magnetic field is generated by a set of triaxial Helmholtz coils described in Ref. [36], with devices rolling on a horizontal plane in the common central workspace, imaged by a top-down camera. For all experiments, the strength of the generated field is 10 mT. The step-out frequency for each device, considered one at a time, is determined experimentally by increasing the rotation frequency of the applied field in increments of 0.05 Hz until an increase in the rotation frequency is found to result in a decrease in the forward velocity, indicating that the prior frequency should be considered the step-out frequency. Thus, the experimentally determined step-out frequency is less than the true step-out frequency, but within 0.05 Hz.

Three experiments [Fig. 8(b) and Ref. [35]] are run to verify the sorting policy. First, "Move all": the group is run at 0.10 Hz, below all of the devices' step-out frequencies, such that all devices rotate synchronously with the field. The total duration of the experiment is 20 s. Second, "Sort 2/3": the fastest two devices (i.e., the two- and three-wire devices) are sorted from the slowest device (i.e., the one-wire device), which remains at the origin. The policy is

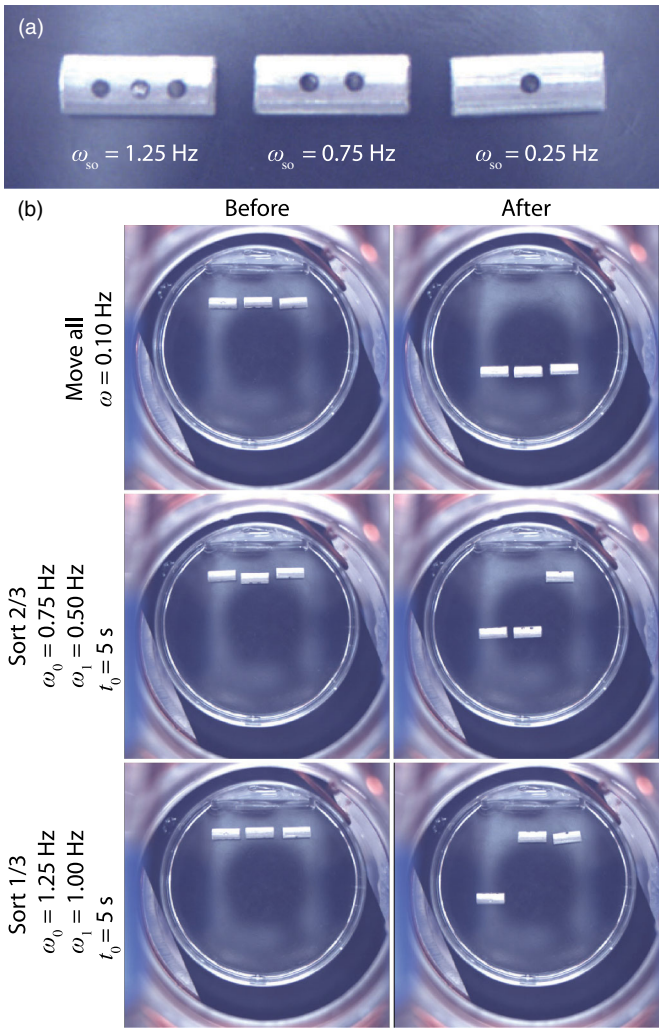

FIG. 8. Experimental verification with three rolling mesomachines [35]. (a) Devices are 3-mm-diameter, 8-mm-long aluminum rods with 0.82-mm-diameter Permalloy 80 wires inserted diametrically. The experimentally determined step-out frequencies in a 2:1 mixture of corn syrup and water are shown. (b) The three possible sorting operations for a three-device group depicted before and after one separation-collection cycle, with the respective parameters shown.

executed with $\omega_0 = 0.75$ Hz, $\omega_1 = 0.50$ Hz, $t_0 = 5$ s, and $n = 1000$ (that is, the policy does not know that there are three devices and assumes there are 1000 devices, effectively converging on the continuous distribution for an arbitrary number of devices). The total duration of the experiment is 7.32 s. Third, "Sort 1/3": the fastest (i.e., three-wire) device is sorted from the two slower devices, which remain at the origin. The sorting policy is executed with $\omega_0 = 1.25$ Hz, $\omega_1 = 1.00$ Hz, $t_0 = 5$ s, and $n = 1000$. The total duration of the experiment is 7.95 s. During selection of policy parameters, ω_0 is chosen to be the minimum step-out frequency in the fast group of devices, and ω_1 is chosen to be the mean of the minimum step-out frequency in the fast group and the maximum

step-out frequency in the slow group. The motion of the devices is captured with a camera, but no feedback is provided to the controller.

V. DISCUSSION

By capitalizing on the magnetic variations between micromachines, we demonstrate a method to sort a select fraction of a group from the remainder and prescribe its net relative movement by implementing open-loop control, instead of relying on the localization information of individual micromachines, which is technologically infeasible in many practical cases. It is important to note that the simulations of Figs. 6 and 7 and the experiments of Fig. 8, which comprise 10, 100, and 3 devices, respectively, all effectively assume a continuous distribution of micromachines (i.e., using $n = 10\,000$ for the simulations, and $n = 1000$ for the experiments).

For a group to be sorted using the technique presented here, the micromachines should possess step-out behavior defined by Eq. (3) and should have approximately identical geometries, and thus hydrodynamic properties. The micromachines in Ref. [5] have magnetic heads attached to nonmagnetic helixes, whereas the micromachines in Refs. [15,37] are nonmagnetic helices with magnetic properties introduced as a thin surface coating, but both meet the necessary requirements to be sorted with the presented techniques by introducing variance in the process that forms the magnetic component. Micromachines without substantially identical geometries would lack the crucial homogeneous operating mode. This deficiency would undermine the most basic group-manipulation primitive of moving the group in unison with $\omega \leq \omega_{\min}$, as well as the separation-collection sorting primitive conceived here.

Variation in the geometry (i.e., β) of a micromachine is directly proportional to relative error in the resulting velocity (and thus displacement) compared to a micromachine with an ideal (mean) geometry. We find that micromachines in the slow group do not exhibit dependence on β during the separation-collection cycle and, consequently, are returned to their original position regardless of geometric variation. As a result, the consequence of variation in geometry is a diffusion in the fast group, with a rms relative error (in displacement) that is identical to the coefficient of variation of β.

The simple low-Reynolds-number swimming model of Sec. II accounts neither for precession nor the effect of gravity nor hydrodynamic and magnetic interactions between micromachines, all of which occur to some degree in actual micromachines. We expect these effects to superimpose with the dynamics described in this paper. As a result, the sorting method presented here should be viewed as one building block toward a complete motion-planning and control system for micromachines, including systems that utilize closed-loop feedback.

Precession already exists in all prior demonstrations of chiral microswimmers, but it does not significantly affect the validity of the model in Eq. (1) in describing the swimming behavior along and around the principal axis of rotation, provided that the microswimmers have a sufficiently high length-to-diameter aspect ratio [34]. Additionally, microswimmers can be designed for stability in order to reduce precession [38]. Unmodeled variation in the orientation of magnetization also contributes to precession in microswimmers, and may be a more significant source of noise in the case of rolling micromachines [10].

Gravity equally affects microswimmers, so any settling or buoyancy effects are not likely to result in significant relative movements between micromachines within the group. Techniques designed for gravity compensation of microswimmers propelled by rotating uniform magnetic fields [36] could likely be superimposed with the techniques described in this paper.

The primary concern, unaccounted for in the model, is the inevitable hydrodynamic and magnetic coupling of neighboring micromachines. Prior experiments have demonstrated small numbers of soft-ferromagnetic chiral microswimmers swimming near each other without experiencing severe parasitic magnetic or hydrodynamic interactions [39], but the micromachines in those experiments were not densely packed. Reference [11] estimates that the unmodeled interactions for this type of micromachine will be negligible for micromachines separated by at least five body lengths but conjectures that the models may retain sufficient validity with denser packing. In experiments with substantially increased density, significant interactions have been observed [16]. In our scaled low-Reynolds-number experiments, shown in Fig. 8(b) and Ref. [35], the mesomachines are in close proximity and there are certainly magnetic and fluidic interactions; yet, in spite of these interactions, three distinct open-loop sorts are demonstrated. At the true microscale, fluidic and magnetic-torque interactions would be equivalent to those of our scaled experiment, but magnetic-force interactions would be relatively larger at the microscale. The interactions of mesomachines with the substrate on which they are rolling will tend to mitigate the effect of unmodeled parasitic forces, and those effects would also be relatively larger at the microscale. Similar benefits will likely be present in the case of micromachines in soft tissue but will not be present in microswimmers in open fluid, and, as a result, they will be more susceptible to drift.

In addition to the unmodeled effects discussed above, the simple low-Reynolds-number swimming model of Sec. II does not account for Brownian motion, which becomes significant for very small devices [11,23]. The model also assumes Newtonian fluid, and it is unclear for what types of biological fluids and tissues the model will be sufficiently predictive, but similar velocity responses to those shown in Fig. 2 have been observed experimentally in soft tissue [4].

Finally, it has been shown that some micromachines in certain scenarios do not exhibit a unique velocity response for a given applied rotating magnetic field [40–42]. In such cases, a certain fraction of the micromachines may have a response that is very poorly described by our modeling assumptions. It is likely that this problem can be mitigated to some degree by prealigning the micromachines (e.g., using a static applied magnetic field) before initiating the field rotation, but it is possible that our method is simply poorly suited to certain types of micromachines.

A remaining open question is how to best develop the statistical distribution of the magnetic properties within the group (see Fig. 3). In our experiments shown in Fig. 8, we experimentally determine the step-out frequencies of each of the three micromachines in isolation, and then we put the group together afterward. For large numbers of micromachines, particularly with an effectively continuous distribution of magnetic properties, it may be desirable to experimentally determine the statistical distribution holistically. For example, the group could be driven at a number of constant frequencies (i.e., separation processes), and the fraction of the group that is fast could be determined [see Fig. 6(b)]. Using such methods, it may even be possible to capture the unmodeled effects discussed above, in a statistical sense.

In the end, there are many possible permutations of micromachine type (e.g., helix, screw, rolling rod, spheroid, achiral swimmers), magnetization type (e.g., permanent magnet, soft magnetic), and environment (e.g., open fluid, tissue) that have the potential to utilize the method described in this paper, each subject to a continuum of micromachine size and concentration. In the limit as the micromachine concentration decreases, we would expect the proposed method to be increasingly accurate. As concentration increases, it is likely that micromachines will not be accurately described by our modeling assumption, and irreversible clumping may even occur. Left as an open question is, for which of the aforementioned scenarios will the proposed method be a sufficiently accurate description of the observed behavior in practice?

ACKNOWLEDGMENTS

This work was supported by the National Science Foundation under Grant No. 1435827. We would like to thank Dr. Henry Fu, as well as the anonymous reviewers; this paper was greatly influenced by their suggestions.

APPENDIX: PROOF OF UNIQUENESS OF COLLECTION PROCESS

An alternative to solving for the collection process $\omega(t)$ is to solve for its inverse, which is a frequency-varying time function: $t(\omega)$. Equation (5) can be reformulated, using the following change of variables:

$$s = t(\Omega), \tag{A1a}$$

$$ds = t'(\Omega)d\Omega, \tag{A1b}$$

$$s = 0 \rightarrow \Omega = \omega_1, \tag{A1c}$$

$$s = t(\omega_{\mathrm{so}}) \rightarrow \Omega = \omega_{\mathrm{so}}, \tag{A1d}$$

as the Volterra integral equation of the first kind:

$$t_0\left(\sqrt{\omega_0^2-\omega_{\mathrm{so}_i}^2}-\sqrt{\omega_0^2-\omega_1^2}\right) = \int_{\omega_1}^{\omega_{\mathrm{so}_i}}\left(\sqrt{\Omega^2-\omega_{\mathrm{so}_i}^2}\right)t'(\Omega)d\Omega, \tag{A2}$$

where the variable of integration is the frequency and $t'(\omega)$ is the first derivative of $t(\omega)$ with respect to the frequency.

We are unable to find a closed-form solution to Eq. (A2). Instead, we solve it numerically by discretizing ω_{so} and Ω, solving for $t'(\omega)$, and then performing the subsequent integration to obtain $t(\omega)$. Both Ω and ω_{so} are discretized over their respective sets:

$$\Omega_i = \omega_1 - \frac{\omega_1}{n}(i-1), \quad i \in [1,n] \rightarrow \Omega \in \left[\omega_1, \frac{\omega_1}{n}\right] \approx [\omega_1, 0], \tag{A3}$$

$$\omega_{\mathrm{so}_j} = \frac{\omega_1}{n}(j-1), \quad j \in [1,n] \rightarrow \omega_{\mathrm{so}} \in \left[0, \left(\frac{n-1}{n}\right)\omega_1\right] \approx [0, \omega_1]. \tag{A4}$$

The right-hand side of Eq. (A2) is discretized as

$$\int_{\omega_1}^{\omega_{\mathrm{so}_j}}\left(\sqrt{\Omega^2-\omega_{\mathrm{so}_j}^2}\right)t'(\Omega)d\Omega \approx \sum_{i=1}^{n} -\left(\sqrt{\Omega_i^2-\omega_{\mathrm{so}_j}^2}\right)t'(\Omega_i)\frac{\omega_1}{n}. \tag{A5}$$

A discretized form of Eq. (A2) is assembled:

$$\mathbf{M}_{ij} = \begin{cases} -\frac{\omega_1}{n}\sqrt{\Omega_i^2-\omega_{\mathrm{so}_j}^2}, & \Omega_i > \omega_{\mathrm{so}_j} \\ 0, & \Omega_i \le \omega_{\mathrm{so}_j} \end{cases}, \tag{A6a}$$

$$\begin{bmatrix} t_0\left(\sqrt{\omega_0^2-\omega_{\mathrm{so}_1}^2}-\sqrt{\omega_0^2-\omega_1^2}\right) \\ \vdots \\ t_0\left(\sqrt{\omega_0^2-\omega_{\mathrm{so}_n}^2}-\sqrt{\omega_0^2-\omega_1^2}\right) \end{bmatrix} = \mathbf{M}\begin{bmatrix} t'(\Omega_1) \\ \vdots \\ t'(\Omega_n) \end{bmatrix}. \tag{A6b}$$

Solve for $t'(\omega)$, then integrate to find $t(\omega)$:

$$t'(\Omega) = \mathbf{M}^{-1}\begin{bmatrix} t_0\left(\sqrt{\omega_0^2-\omega_{\mathrm{so}_1}^2}-\sqrt{\omega_0^2-\omega_1^2}\right) \\ \vdots \\ t_0\left(\sqrt{\omega_0^2-\omega_{\mathrm{so}_n}^2}-\sqrt{\omega_0^2-\omega_1^2}\right) \end{bmatrix}, \quad \text{(A7a)}$$

$$t(\omega) = \int_{\omega_1}^{0} t'(\Omega)d\Omega. \quad \text{(A7b)}$$

The invertibility of $\mathbf{M}$ proves the collection process is unique (given a constant-frequency separation process).

[1] S. Chowdhury, W. Jing, and D. J. Cappelleri, Controlling multiple microrobots: Recent progress and future challenges, J. Micro-Bio Rob. **10**, 1 (2015).

[2] M. Sitti, H. Ceylan, W. Hu, J. Giltinan, M. Turan, S. Yim, and E. Diller, Biomedical applications of untethered mobile milli/microrobots, Proc. IEEE **103**, 205 (2015).

[3] B. J. Nelson, I. K. Kaliakatsos, and J. J. Abbott, Microrobots for minimally invasive medicine, Annu. Rev. Biomed. Eng. **12**, 55 (2010).

[4] K. Ishiyama, M. Sendoh, A. Yamazaki, and K. I. Arai, Swimming micro-machine driven by magnetic torque, Sens. Actuators A **91**, 141 (2001).

[5] L. Zhang, J. J. Abbott, L. X. Dong, B. E. Kratochvil, D. Bell, and B. J. Nelson, Artificial bacterial flagella: Fabrication and magnetic control, Appl. Phys. Lett. **94**, 064107 (2009).

[6] A. Ghosh and P. Fischer, Controlled propulsion of artificial magnetic nanostructured propellers, Nano Lett. **9**, 2243 (2009).

[7] E. Diller, S. Floyd, C. Pawashe, and M. Sitti, Control of multiple heterogeneous magnetic microrobots in two dimensions on nonspecialized surfaces, IEEE. Trans. Robot. **28**, 172 (2012).

[8] E. Diller, J. Giltinan, and M. Sitti, Independent control of multiple magnetic microrobots in three dimensions, Int. J. Rob. Res. **32**, 614 (2013).

[9] T.-Y. Huang, F. Qiu, H.-W. Tung, K. E. Peyer, N. Shamsudhin, J. Pokki, L. Zhang, X.-B. Chen, B. J. Nelson, and M. S. Sakar, Cooperative manipulation and transport of microobjects using multiple helical microcarriers, RSC Adv. **4**, 26771 (2014).

[10] P. Mandal, V. Chopra, and A. Ghosh, Independent positioning of magnetic nanomotors, ACS Nano **9**, 4717 (2015).

[11] P. J. Vach, S. Klumpp, and D. Faivre, Steering magnetic micropropellers along independent trajectories, J. Phys. D **49**, 065003 (2016).

[12] M. Salehizadeh and E. Diller, Two-agent formation control of magnetic microrobots in two dimensions, J. Micro-Bio Rob. **12**, 9 (2017).

[13] J. Rahmer, C. Stehning, and B. Gleich, Spatially selective remote magnetic actuation of identical helical micromachines, Sci. Rob. **2**, eaal2845 (2017).

[14] S. Tottori, L. Zhang, K. E. Peyer, and B. J. Nelson, Assembly, disassembly, and anomalous propulsion of microscopic helices, Nano Lett. **13**, 4263 (2013).

[15] A. Servant, F. Qiu, M. Mazza, K. Kostarelos, and B. J. Nelson, Controlled *in vivo* swimming of a swarm of bacteria-like microrobotic flagella, Adv. Mater. **27**, 2981 (2015).

[16] P. J. Vach, D. Walker, P. Fischer, P. Fratzl, and D. Faivre, Pattern formation and collective effects in populations of magnetic microswimmers, J. Phys. D **50**, 11LT03 (2017).

[17] J. J. Abbott, K. E. Peyer, M. Cosentino Lagomarsino, L. Zhang, L. Dong, and B. J. Nelson, How should microrobots swim?, Int. J. Rob. Res. **28**, 1434 (2009).

[18] K. Ishiyama, M. Sendoh, and K. I. Arai, Magnetic micromachines for medical applications, J. Magn. Magn. Mater. **242**, 41 (2002).

[19] S. Tottori, N. Sugita, R. Kometani, S. Ishihara, and M. Mitsuishi, Selective control method for multiple magnetic helical microrobots, J. Micro-Nano Mechatron. **6**, 89 (2011).

[20] U. K. Cheang, K. Lee, A. A. Julius, and M. J. Kim, Multiple-robot drug delivery strategy through coordinated teams of microswimmers, Appl. Phys. Lett. **105**, 083705 (2014).

[21] A. W. Mahoney, N. D. Nelson, K. E. Peyer, B. J. Nelson, and J. J. Abbott, Behavior of rotating magnetic microrobots above the step-out frequency with application to control of multi-microrobot systems, Appl. Phys. Lett. **104**, 144101 (2014).

[22] D. Cappelleri, D. Efthymiou, A. Goswami, N. Vitoroulis, and M. Zavlanos, Towards mobile microrobot swarms for additive micromanufacturing, Int. J. Adv. Rob. Syst. **11**, 150 (2014).

[23] P. J. Vach, N. Brun, M. Bennet, L. Bertinetti, M. Widdrat, J. Baumgartner, S. Klumpp, P. Fratzl, and D. Faivre, Selecting for function: Solution synthesis of magnetic nanopropellers, Nano Lett. **13**, 5373 (2013).

[24] D. Schamel, M. Pfeifer, J. G. Gibbs, B. Miksch, A. G. Mark, and P. Fischer, Chiral colloidal molecules and observation of the propeller effect, J. Am. Chem. Soc. **135**, 12353 (2013).

[25] M. Mijalkov and G. Volpe, Sorting of chiral microswimmers, Soft Matter **9**, 6376 (2013).

[26] Marcos, H. C. Fu, T. R. Powers, and R. Stocker, Separation of Microscale Chiral Objects by Shear Flow, Phys. Rev. Lett. **102**, 158103 (2009).

[27] A. Becker, C. Onyuksel, T. Bretl, and J. McLurkin, Controlling many differential-drive robots with uniform control inputs, Int. J. Rob. Res. **33**, 1626 (2014).

[28] T. Bretl, Minimum-time optimal control of many robots that move in the same direction at different speeds, IEEE. Trans. Robot. **28**, 351 (2012).

[29] E. M. Purcell, Life at low Reynolds number, Am. J. Phys. **45**, 3 (1977).

[30] K. I. Morozov and A. M. Leshansky, The chiral magnetic nanomotors, Nanoscale **6**, 1580 (2014).

[31] B. H. McNaughton, K. A. Kehbien, J. N. Anker, and R. Kopelman, Sudden breakdown in linear response of a rotationally driven magnetic microparticle and application to physical and chemical microsensing, J. Phys. Chem. B **110**, 18958 (2006).

[32] P. Tierno, J. Claret, F. Sagués, and A. Cēbers, Overdamped dynamics of paramagnetic ellipsoids in a precessing magnetic field, Phys. Rev. E **79**, 021501 (2009).

[33] V. M. Fomin, E. J. Smith, D. Makarov, S. Sanchez, and O. G. Schmidt, Dynamics of radial-magnetized microhelix coils, Phys. Rev. B **84**, 174303 (2011).

[34] A. Ghosh, P. Mandal, S. Karmakar, and A. Ghosh, Analytical theory and stability analysis of an elongated nanoscale object under external torque, Phys. Chem. Chem. Phys. **15**, 10817 (2013).

[35] See Supplemental Material at http://link.aps.org/supplemental/10.1103/PhysRevApplied.9.054021 for video of experimental verification with three rolling mesomachines.

[36] A. W. Mahoney, J. C. Sarrazin, E. Bamberg, and J. J. Abbott, Velocity control with gravity compensation for magnetic helical microswimmers, Adv. Rob. **25**, 1007 (2011).

[37] S. Tottori, L. Zhang, F. Qiu, K. K. Krawczyk, A. Franco-Obregón, and B. J. Nelson, Magnetic helical micromachines: Fabrication, controlled swimming, and cargo transport, Adv. Mater. **24**, 811 (2012).

[38] H. C. Fu, M. Jabbarzadeh, and F. Meshkati, Magnetization directions and geometries of helical microswimmers for linear velocity-frequency response, Phys. Rev. E **91**, 043011 (2015).

[39] L. Zhang, J. J. Abbott, L. Dong, K. E. Peyer, B. E. Kratochvil, H. Zhang, C. Bergeles, and B. J. Nelson, Characterizing the swimming properties of artificial bacterial flagella, Nano Lett. **9**, 3663 (2009).

[40] A. Ghosh, D. Paria, H. J. Singh, P. L. Venugopalan, and A. Ghosh, Dynamic configuration and bistability of helical nanostructures under external torque, Phys. Rev. E **86**, 031401 (2012).

[41] F. Meshkati and H. C. Fu, Modeling rigid magnetically rotated microswimmers: Rotation axes, bistability, and controllability, Phys. Rev. E **90**, 063006 (2014).

[42] K. I. Morozov, Y. Mirzae, O. Kenneth, and A. M. Leshansky, Dynamics of arbitrary shaped propellers driven by a rotating magnetic field, Phys. Rev. Fluids **2**, 044202 (2017).